ACS OMEGA

http://pubs.acs.org/journal/acsodf

Article

Spray-Based Method for Protecting and Restoring Historic Adobe Walls Using Nanomontmorillonite Clay

Mona Khaksar, Hamed Niroumand,* Maryam Afsharpour, and Lech Balachowski

Cite This: *ACS Omega* 2023, 8, 11373−11380

Read Online

ACCESS | Metrics & More | Article Recommendations

ABSTRACT: Restoring and protecting historic buildings worldwide are important because heritage buildings are records of the civilizations of various countries. Herein, nanotechnology was used to restore historic adobe walls. According to the Iran Patent and Trademark Office (IRPATENT) 102665, nanomontmorillonite clay has been selected as a natural and compatible material with adobe. Furthermore, it has been used as nanospray to be a minimally invasive method to fill cavities and cracks in the adobe surface. Various percentages of nanomontmorillonite clay (1−4%) in the ethanol solvent and the frequency of spraying on the wall surface were evaluated. Scanning electron microscopy and atomic force microscopy images, porosity tests, water capillary absorption, and compressive strength tests were used to evaluate the efficiency of the method, analyze cavity filling, and detect the optimal percentage of nanomontmorillonite clay. Results indicate that the double use of the 1% nanomontmorillonite clay solution exhibited the best results, filled the cavities, and reduced the pores on the surface of the adobe, increasing compressive strength and reducing water absorption and hydraulic conductivity. The use of a more dilute solution causes the nanomontmorillonite clay to penetrate deeply into the wall. This innovative method can help mitigate the existing disadvantages of historic adobe walls.

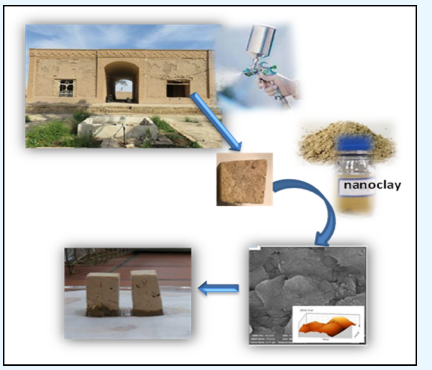

1. INTRODUCTION

Masonry materials have been used in construction for thousands of years. Approximately 30−40% of the world's population lives in houses constructed using earth materials. Most of the earth's remaining or endangered cultural structures have been constructed using various techniques that consider the materials used in construction and their compositions. These structures are subject to erosion and scaling owing to precipitation during moisture and salt removal. Moreover, they can crack under the slightest tensile and compressive stresses.[1,2] Because masonry materials are nonhomogeneous compounds, with an increase in environmental pollution along with the weathering process, particularly in historic buildings, changes occur in the structures of their raw materials. These changes mostly manifest in the form of surface damage, particularly at mortar joints.[3,4]

Considering long-term durability, recyclability, and workability with the least amount of energy and the use of environmentally friendly materials, the focus on brick buildings in sustainable constructions is increasing. Adobe is a primary brick that contains soil (clay, sand, and gravel) and water and dries owing to prolonged exposure to sunlight. In mentioned materials, straws and fibers are used to prevent cracking.[5] The amount of clay in adobe blocks considerably affects the amount of moisture in walls.[6] Additionally, the amount of granulation and adhesion of soil affect the rate of clay erosion and the type of clay mineral and soluble and insoluble salts in the soil.[7]

Soil properties that can help enhance mechanical properties, reduce volumetric changes caused by water infiltration, and increase resistance to wind and rain erosion can be improved using three methods of mechanical stabilization: (1) soil compaction for changing mechanical parameters, (2) physical stabilization involving changes in properties and soil texture by adding materials such as fibers, and (3) chemical stabilization by adding materials such as cement, lime, bitumen, or chemicals.[8,9]

The presence of cracks in clay affected by the shrinkage caused by drying increases hydraulic conductivity. Compacted clay can be used as a barrier to hydraulic conductivity.[10] To strengthen and enhance the service life of historic buildings, periodic interventions are important to maintain the structure and function of these buildings. These compacted clay techniques should be noninvasive and stable to preserve them.[11] Retrofitting methods are divided into forms of

Received: January 7, 2023
Accepted: March 8, 2023
Published: March 16, 2023

conservation, preservation, rehabilitation, restoration, and maintenance.[12] For any monument, selecting the method of the intervention method is a complex choice owing to the lack of sufficient information regarding the monument structure, including structural features, material knowledge, geometric data, construction type, and monument management.[13] Owing to competition concerning the use of innovative and consistent methods for protecting historic monuments, most studies in the field of creating multipurpose coatings on the surfaces of historic buildings are based on two approaches: (1) improving the durability of traditional materials and (2) reducing interventions and cost. Moreover, the use of nanotechnology in reducing or preventing the presence of harmful factors has been considered.[14]

Recently, studies on various applications of nanoparticles in various fields of architecture and civil engineering, particularly in soil stabilization, and on improving the properties of building materials have become extensive. Various nanomaterials have been used to achieve soil stabilization. Several studies have shown that adding nanoparticles to soil improves the geotechnical properties of the soil.[15] For instance, nano-SiO_2 helps improve the geotechnical properties of cohesive soil.[16] Moreover, nanotechnology studies in the field of cultural heritage include investigating the surfaces of historic stones and bricks and creating photocatalytic layers using TiO_2.[17,18]

Nanoclays are considered common commercial nanomaterials. These nanoparticles, which are obtained by repeatedly filtering clay powders, possess high resistance to ultraviolet light and heat owing to their high aspect ratios.[19,20] Studies on the effect of nanomontmorillonite clay on soil permeability have shown that the addition of nanoclays reduces the permeability and swelling of soils.[21,22] Moreover, these studies indicate that the combination of nanomaterials with nanoclays affects the behavior of soils vulnerable to landslides.[23] Furthermore, addition of clay nanoparticles to the soil reduces the hydraulic conductivity of the soil.[24−26] Various studies have demonstrated the effectiveness of using nanoclays to increase the strength of soil.[27−29] Nanoclays and glass fibers play an important role in reducing soil density by covering fiber surfaces with nanoclays, which helps in considerably reducing the fine cracks on the mixture surface and increasing the shear strength of the soil.[30] The use of soil is common in construction; however, the low strength and high density of soil have necessitated the use of techniques that can improve soil properties. Furthermore, using such techniques, the strength, compressibility, and hydraulic conductivity of soil can be improved.[31] Nanoclay increased the yield stress in cementation systems because it could fill void spaces.[34] Montmorillonite is a type of clay. Nanomontmorillonite plays an important role in improving thixotropy.[33]

Various studies on the use of diverse nanoparticles, particularly nanoclays, for soil stabilization have been conducted; however, till date, these nanoadditives have not been used for restoring and protecting adobe buildings using spray-based methods. This study investigates the coating effect of montmorillonite clay nanoparticles on historical adobe walls. Hot and dry weather conditions cause surface erosion and hair cracks in historic adobe walls, degrading adobe walls and historic buildings in various countries.

2. MATERIALS AND TESTING PROCEDURE

2.1. Materials. The historic adobe walls considered herein were selected from the Kashani historical monument in Padeh village, Semnan province, Iran. Kashani house was built in (1948 BC) 1328 AD in the first Pahlavi period using adobe and brick materials. Herein, the basic adobes with dimensions of 25 cm × 25 cm × 5 cm were cut to dimensions of 5 cm × 5 cm × 5 cm in accordance with the minimum laboratory requirement. According to IRPATENT 102665,[32] nanomontmorillonite clay was used herein. The density of nanomontmorillonite clay (produced by Sigma Aldrich (USA) under the brand name of MontmorilloniteK10) ranged from 0.5 to 0.7 gr/cm^3, and its particle size ranged from 1 to 2 nm. Moreover, this nanoclay comprised 50.95% SiO_2 and 19.6% AL_2O_3, with the remainder composition of Fe_2O_3, MgO, CaO, Na2O, K_2O, and TiO_2.

2.2. Samples. To achieve the optimal ratio of nanomontmorillonite in the spray, weight-to-volume ratios of 1, 2.5, and 4% w/v of nanomontmorillonite clay in the ethanol solvent were investigated. After weighing, the desired amounts of nanomontmorillonite clay were mixed with 100 mL of the ethanol solvent and placed in an ultrasonic bath for 30 min. Each solution (100 mL) was sprayed on the sample surface with an area of 180 cm^2 (Figure 1). Seven samples with dimensions of 5 cm × 5 cm × 5 cm were considered for this study. Various percentages of nanomontmorillonite clay were sprayed on all the sample surfaces and tested in four categories (First sample: non-nanomontmorillonite clay as the control sample = Cc, 1% nanomontmorillonite clay = C1, 2.5% nanomontmorillonite clay = C2.5, and 4% nanomontmorillonite clay = C4).

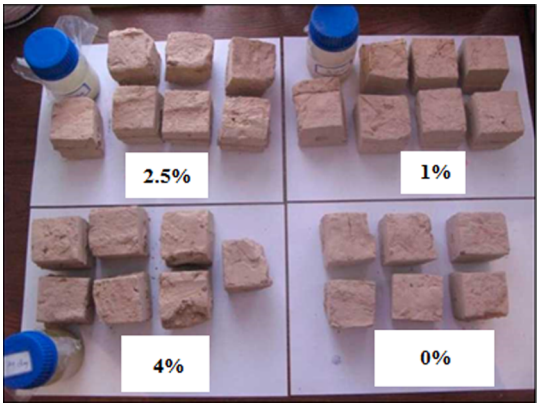

Figure 1. Preparation of samples for spraying nanomontmorillonite clay.

2.3. Tests. The optimal percentage of nanomontmorillonite clay was determined on the basis of the comparison of pore filling in all the samples by conducting a field-emission scanning electron microscopy/scanning electron microscopy (FESEM/SEM) test using the MIRA3TESCAN-XMU model and the atomic force microscopy (AFM) test using the DME-95-50 E model. For the uniaxial compressive strength test, samples with dimensions of 5 mm × 15 mm × 25 mm were prepared and two clay samples were tested before and after spraying. To measure porosity in historical samples, a gas porosity method was selected. Samples with dimensions of 45 mm × 20 mm × 20 mm were prepared; three samples were prepared for test validation. This test was performed using the PO-R30 model. This model does not damage the sample and uses nitrogen gas. The hydraulic conductivity test was performed using an oven. For this test, samples with

https://doi.org/10.1021/acsomega.3c00124
ACS Omega 2023, 8, 11373−11380

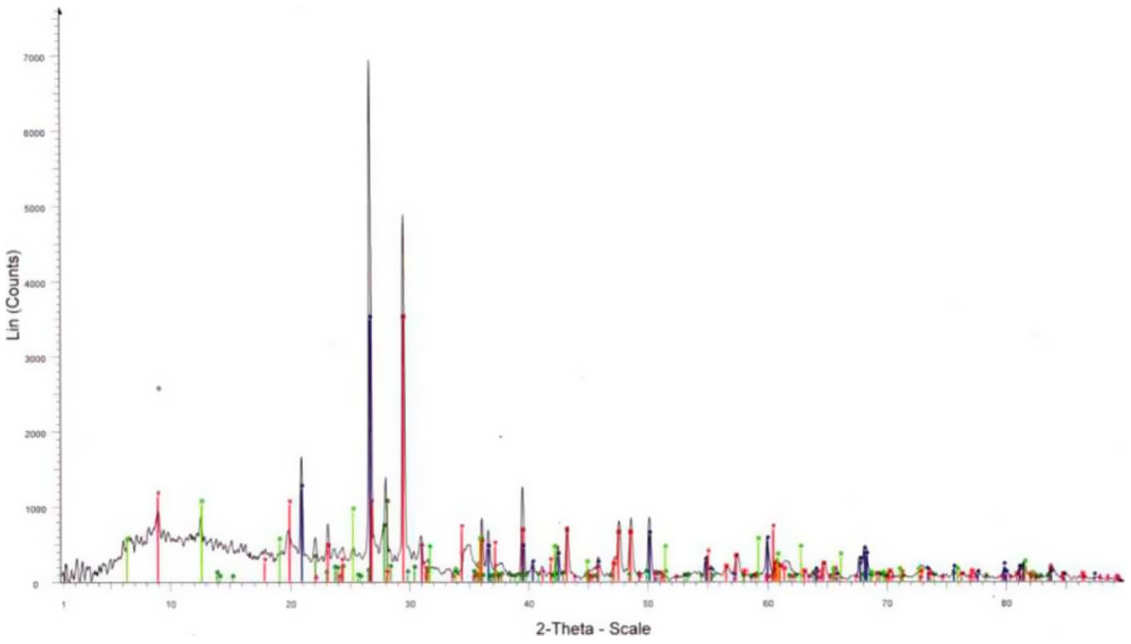

Figure 2. X-ray diffraction pattern for the control sample.

approximate dimensions of 20 mm × 20 mm × 45 mm were prepared. The control and sprayed samples were initially weighed and subsequently placed in an oven at 80 °C for 24 h for moisture evaporation and complete drying. After cooling the samples, a piece of foam with a thickness of 1 cm and a thin cloth were placed on them. Water was added to a container according to the thickness of the foam. Subsequently, the samples were placed in the container at an interval of 5 s. Finally, the weight of the samples was measured on the basis of the amount of absorbed water. Moreover, a compressive strength test was performed. Samples with dimensions of 5 cm × 5 cm × 5 cm were prepared for the Unconfined Compressive Strength (UCS).

3. RESULTS AND DISCUSSION

3.1. Recognizing the Historic Adobe. Figure 2 shows the X-ray diffraction pattern of historical clay. As can be seen, adobe comprises quartz (SiO_2), calcite ($CaCO_3$), feldspar (Na and Ca), clay minerals, and dolomite ($CaMg(CO_3)_2$). Figure 3 shows the amount of nitrogen uptake and the desorption curve. Figure 4 shows the pore-size distribution of historic adobe samples. Results show a specific surface area of 20.088 m^2/g, total pore volume of 0.079 cm^3/g, and mean pore diameter of 15.87 nm. Based on the pore-size distribution curve, most pores were <4 nm in size. Figure 5 shows the SEM

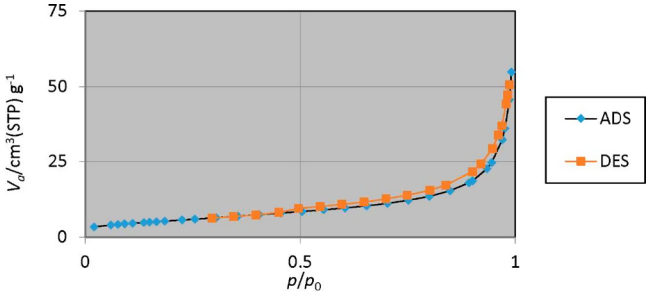

Figure 3. Nitrogen adsorption and desorption curves.

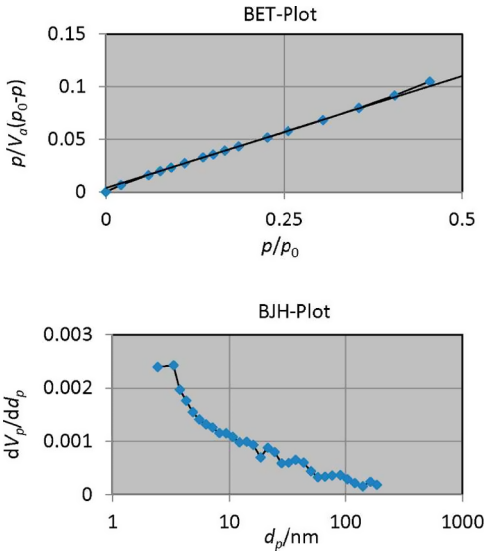

Figure 4. Brunauer–Emmett–Teller and Barrett–Joyner–Halenda curves of the control sample.

image of the clay; the surface erosion of clay is visible in the form of pores and cracks on the surface.

3.2. Coating Historical Adobe with Spray-Based Nanomontmorillonite Clay. Herein, various tests were performed concerning the protection of coated and noncoated adobe samples.

3.2.1. Scanning Electron Microscopy. Initially, the SEM test was performed on samples. Figure 6 shows the control samples and spray-based adobe samples with 1, 2.5, and 4% nanomontmorillonite clay, and Figure 7 shows the SEM images of the samples.

Figure 6 shows a layer of nanomontmorillonite clay on the adobe surface. Hairline cracks were observed in the 1% sample; however, in the 2.5% sample, a uniform and covered surface of nanomontmorillonite clay was observed. In some parts, the accumulation of nanomontmorillonite clay and reduction of

https://doi.org/10.1021/acsomega.3c00124
ACS Omega 2023, 8, 11373−11380

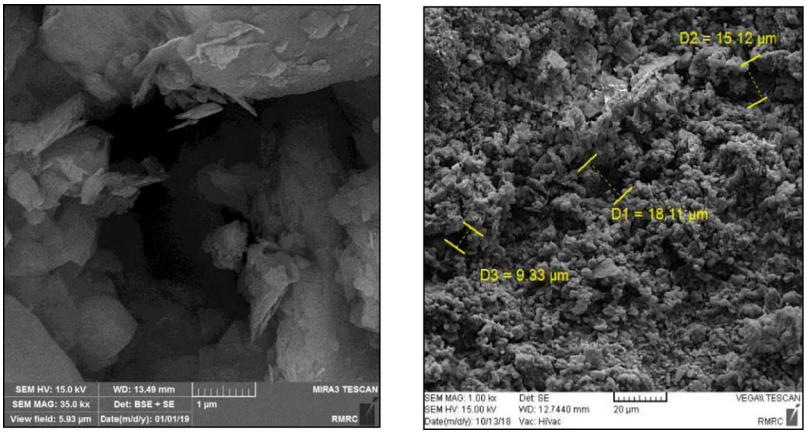

Figure 5. SEM image of the control sample.

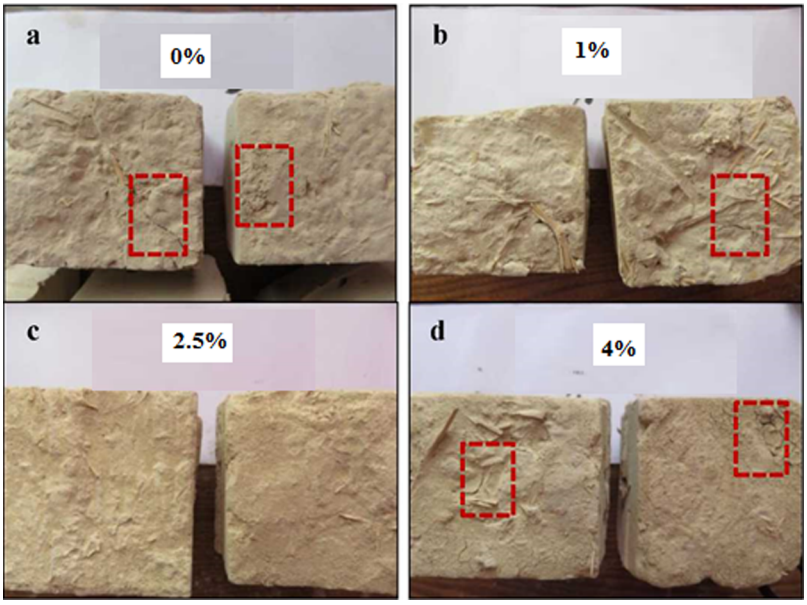

Figure 6. Intuitive evaluations of the (a) control sample, (b) sample sprayed with 1% nanomontmorillonite clay solution (C1), (c) sample sprayed with 2.5% nanomontmorillonite clay solution (C2.5), and (d) sample sprayed with 4% nanomontmorillonite clay solution (C4).

adsorption were observed. In the 4% sample, a complete increase in new hairline cracks was observed.

A comparison of the SEM images of the sprayed samples (Figure 7) with that of the control sample (Figure 5) shows a uniform surface of nanomontmorillonite clay cover and cavity filling in 1 and 2.5% samples; however, the crack distance in the 2.5% sample is less than that in the 1% sample. In the 4% sample, the accumulation of nanomontmorillonite clay particles in the form of the increased number of cavities is evident.

Based on the obtained images, the 4% sample was rejected owing to the increase in the number of cavities and cracks and was subjected only to a pressure test. However, in the 1% sample, a space existed for clay-nanoparticle penetration. However, in the 2.5% sample, the pores were filled under good conditions, indicating the importance of penetration using the spray-based method. Therefore, to achieve more accurate results, C1 samples were sprayed again with a layer comprising the same percentage of nanomontmorillonite clay. In this case, the nanomontmorillonite clay percentage of C1 samples was closer to that of C2.5 samples. Figure 8 shows the highly magnified FESEM images of 1% spray and 1% double spray.

According to Figure 8, the double use of 1% nanomontmorillonite clay solution in the spray application process compared with the 2.5% sample exhibited greater penetration into the smallest pores in the adobe owing to its thickness. Thus, it exhibited a suitable coverage effect. Therefore, the spray-based method was repeated twice, and 1% of the nanomontmorillonite clay solution in each spray was selected as the optimum value.

3.2.2. Determination of Porosity Percentages Based on the Gas Porosity Method. Table 1 lists the percentages of control porosity. The obtained data indicate that despite the filling of adobe cavities with nanomontmorillonite clay, the porosity of the samples increased. First, the gas porosity test was performed by penetrating the gas into the sample using a spray-based technique. Subsequently, the existing porosity was calculated. The reason for the increase in porosity can be attributed to the very small nanomontmorillonite clay cavities coated on the surface.

https://doi.org/10.1021/acsomega.3c00124
ACS Omega 2023, 8, 11373−11380

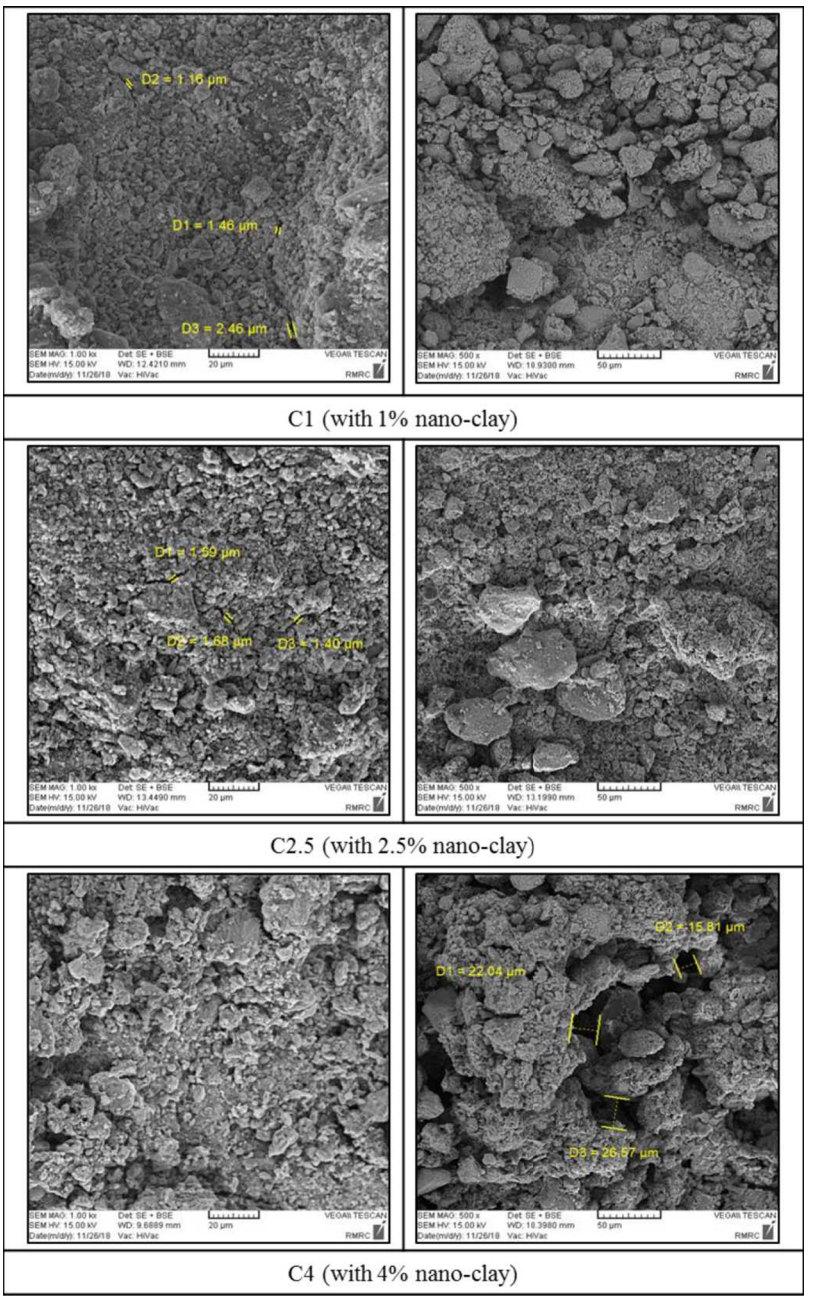

Figure 7. SEM images of the three types of adobe after spraying.

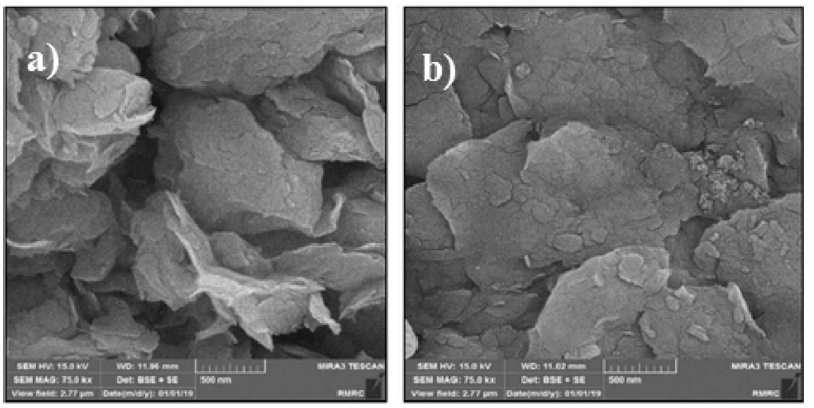

Figure 8. Sample FESEM images: (a) 1% with one-stage spray; (b) 1% with two-stage spray.

https://doi.org/10.1021/acsomega.3c00124
ACS Omega 2023, 8, 11373−11380

Table 1. Porosity Percentage in the Control and Optimal Samples

	porosity average (%)	
	control sample	optimum sample
test 1	39.97	42.31
test 2	45.68	46.35
test 3	38.41	40.98

3.2.3. Surface Analysis Using the AFM Method. The three-dimensional image of the control sample (Figure 9a), depicting a scanned area of 5 μm × 5 μm, shows that the depth of the holes in the sample was 9 μm. Moreover, there were several raised and sunken points, indicating a lack of surface smoothness. According to the obtained graph, cavities with a depth of 400 nm could be observed at a distance of 200 nm. By reducing the dark spots, achieving a uniform level was possible.

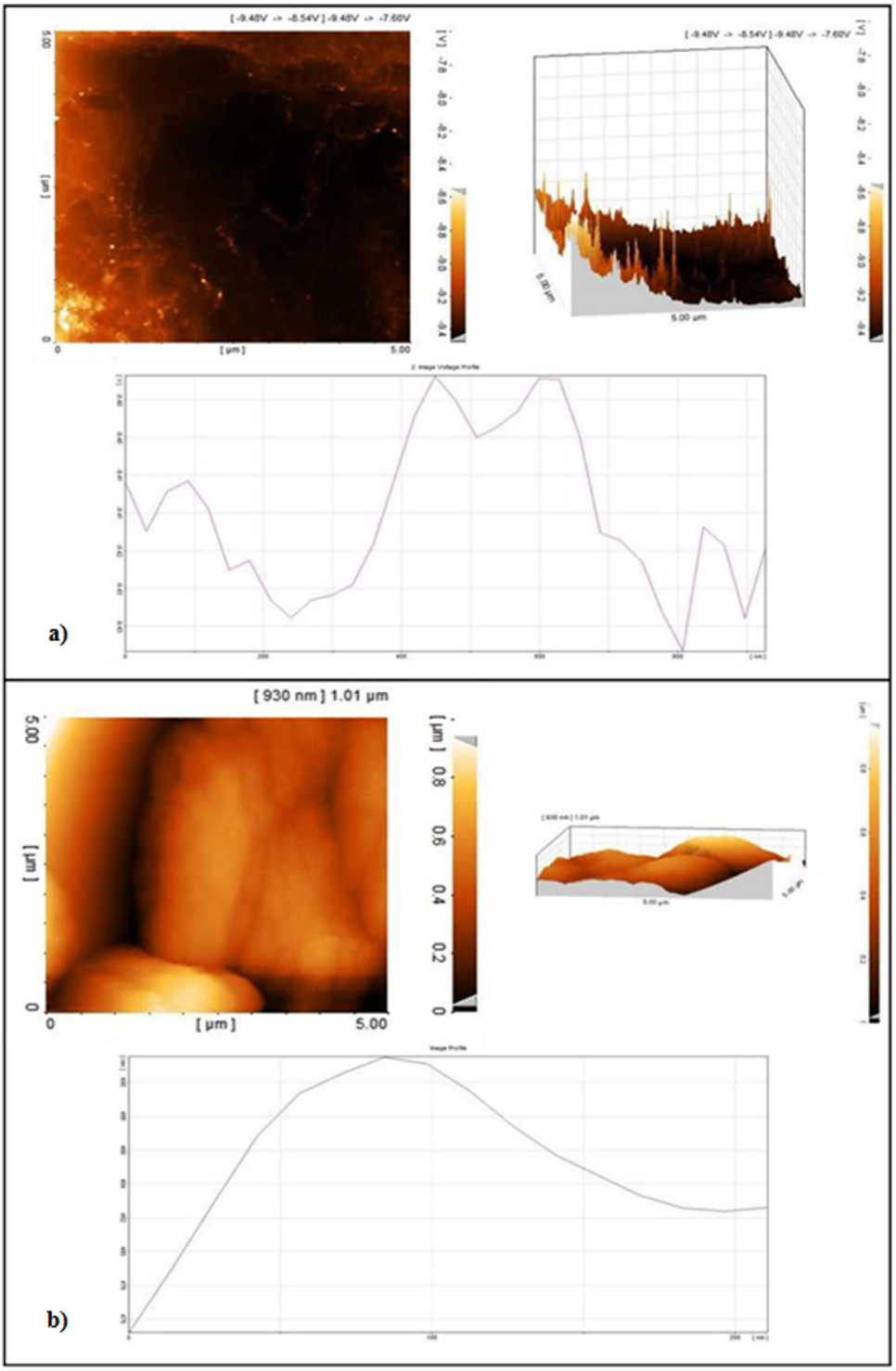

Figure 9. AFM of the (a) control and (b) optimal samples.

https://doi.org/10.1021/acsomega.3c00124
ACS Omega 2023, 8, 11373−11380

The nanomontmorillonite clay particles penetrate larger spaces and fill cavities.

3.2.4. Effect of Nanomontmorillonite Clay Spray on Hydraulic Conductivity. Figure 10 shows the control and

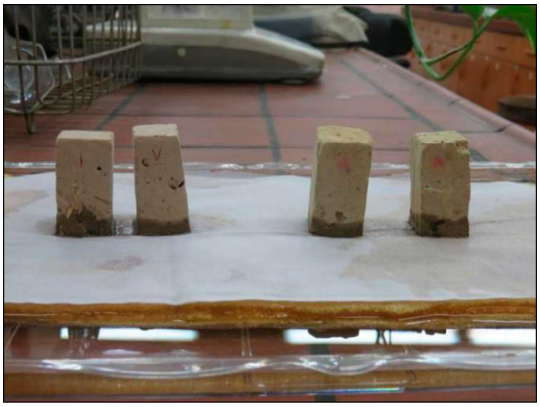

Figure 10. Hydraulic conductivity test.

Table 2. Results Showing the Sample Weight and Saturation Time Obtained during the Capillary Absorption Test

samples	initial weight of the sample (gr)	weight of the samples after drying (gr)	weight of the samples after saturation (gr)	difference in the weight of saturated and dry state (gr)	saturation time (min)
control sample 1	38.1	37.77	49.74	11.97	220
control sample 2	36.6	36.27	50.39	14.12	160
optimum sample 1	37.4	37.12	46.49	9.37	275
optimum sample 2	34.6	34.42	47.3	12.88	140

optimal samples of the hydraulic conductivity test. Table 2 lists the changes in the weight and duration of the saturation of the samples. The filling of larger cavities in the optimal specimens reduced the water flow rate, increasing the water uptake time and reducing the hydraulic conductivity. Moreover, according to the obtained observations, in the control samples, after 10 min, crushing and cracking behaviors were observed in the lower part of the samples, whereas these behaviors appeared in the case of the optimal samples after 50 min.

3.2.5. Effect of Nanomontmorillonite Clay Spray on Compressive Strength. Figure 11 shows the results of the compressive strength test for all the sprayed samples compared with the control sample. In all the sprayed samples, owing to the filling of cavities and reduction in the number of voids, the compressive strength of the samples increased.

4. CONCLUSIONS

Herein, the effect of nanomontmorillonite clay particles on historical adobe walls was investigated based on the results of FE-SEM, AFM, and porosity tests; hydraulic conductivity; and compressive strength. The images obtained from the FESEM and AFM tests showed that using the spray-based method, nanomontmorillonite clay particles filled the pores by penetrating the empty space of the adobe, reduced the diameter of the cavities, and created a uniform layer on the

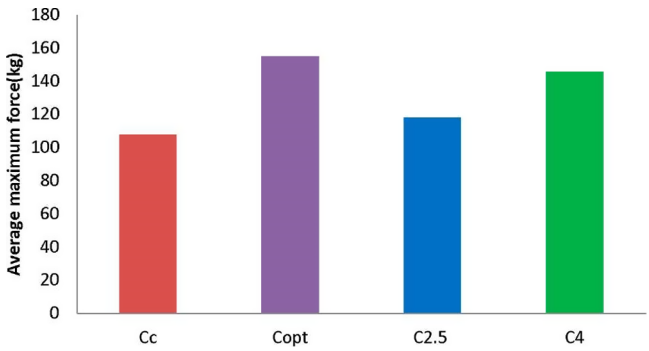

Figure 11. Maximum compressive strength applied to the samples.

surface of the adobe. The optimal amount of nanomontmorillonite clay particles was sprayed twice as a 1% solution, increasing the compressive strength up to 44% compared with the nonsprayed samples. Moreover, in the context of the investigation of the resistance effect of optimal samples against moisture, hydraulic conductivity reduced by 14% compared with the control adobe. In all the sprayed samples, owing to the filling of cavities and reduction in the number of voids, the compressive strength of the samples increased.

Herein, the effect of nanomontmorillonite clay particles on historic buildings considering the spray-based technique was expressed as an innovative and effective method for protecting and restoring historic buildings composed of adobe. Furthermore, this method can be used to protect and restore other soil materials, bricks, or rammed earth walls.

Future work will involve a further implementation of various nanoadditives to evaluate the contribution of the different disadvantages and various climate changes included in historic buildings. The main aim is to protect various types of historic buildings such as adobe, cob, bricks, rammed earth, and heritage because they show the civilization and culture of various countries.

AUTHOR INFORMATION

Corresponding Author

Hamed Niroumand − *Department of Civil Engineering, Faculty of Engineering, Buein Zahra Technical University (IKIU-BZ), Qazvin 34149, Iran;* orcid.org/0000-0001-7765-9581; Email: niroumand.mrud@gmail.com, niroumand@bzeng.ikiu.ac.ir

Authors

Mona Khaksar − *Department of Conservation and Restoration, Faculty of Architecture, Islamic Azad University Central Tehran Branch, Tehran 90234, Iran*

Maryam Afsharpour − *Department of Inorganic Chemistry, Chemistry and Chemical Engineering Research Center of Iran, Tehran 67824, Iran*

Lech Balachowski − *Department of Geotechnical and Hydraulic Engineering, Faculty of Civil and Environmental Engineering, Gdansk University of Technology, Gdansk 80-233, Poland*

Complete contact information is available at: https://pubs.acs.org/10.1021/acsomega.3c00124

Notes

The authors declare no competing financial interest.

https://doi.org/10.1021/acsomega.3c00124
ACS Omega 2023, 8, 11373−11380

■ ACKNOWLEDGMENTS

The authors acknowledge the financing of the Polish National Agency for Academic Exchange.

■ REFERENCES

(1) Micolli, L.; Muller, U.; Fontana, P. Mechanical behaviour of earthen materials: A comparison between earth block masonry, rammed earth and cob. *Constr. Build. Mater.* **2014**, *61*, 327−339.
(2) Craterre building cultture and sustainable development, http://craterre.org/enseignement?new_lang=en_GB
(3) Honeyborne, D. B. Weathering and decay of masonry. In *Conservation of Building and Decorative Stone*, Ashurst, J., Dimes, F. G.; Butterworth-Heinemann Series in Conservation and Museology, Vol. *1*; T&F Group: London, 1990.
(4) Amoroso, G. G., Fassina, V. *Stone decay and conservation; Atmospheric pollution, cleaning; and consolidation*; Elsevier: New York, 1983; p. 453.
(5) Calabria, J. A.; Vasconcelos, W. L.; Boccaccini, A. R. Microstructure and chemical degradation of adobe and clay bricks. *Ceram. Int.* **2009**, *35*, 665−671.
(6) Burroughs, S. Soil property criteria for rammed earth stabilization. *J. Mater. Civ. Eng.* **2008**, *20*, 264−273.
(7) Watanabe, K., Vatandoust, R., Okada, Y. Physical, mineralogical and chemical properties of mudbrick of the Choga Zanbi. In *9th Internaional conference on the study and conservation of earthen architecture-Terra*, Yazd, Iran, 2002.
(8) Houben, H.; Balderrama, A. A.; Simon, S. Our Earthen Architectural Heritage: Materials Research and Conservation. *MRS Bull.* **2004**, *29*, 338−341.
(9) Qiang, X.; Hai-jun, L.; Zhen-ze, L.; Lei, L. Cracking, water permeability and deformation of compacted clay liners improved by straw fiber. *Eng. Geol.* **2014**, *178*, 82−90.
(10) Coo, J.; So, Z. P. S.; Ng, C. W. W. Effect of nanoparticles on the shrinkage properties of clay. *Eng. Geol.* **2016**, *213*, 84−88.
(11) The Athens charter for the restoration of historic monuments. In *Athens Conference*, 1931.
(12) Korkmaz, E.; Vatan, M. Retrofitting Deniz Palace Historic Building for Reusing. *Int. J. Mech. Mechatron. Eng.* **2012**, *2*, 269−278.
(13) Colonna, M.; Gentilini, C.; Pratico, F.; Ubertini, F. Surface Treatments for Historical Constructions Using Nanotechnology. *Key Eng. Mater.* **2014**, *624*, 313−321.
(14) Quagliarini, E.; Bondioli, F.; Goffredo, G. B.; Licciulli, A.; Munafo, P. Self-cleaning materials on Architectural Heritage: Compatibility of photo-induced hydrophilicity of TiO2 coatings on stone surfaces. *J. Cult. Herit.* **2013**, *14*, 1−7.
(15) Ghasabkolaei, N.; Choobbasti, A. J.; Roshan, N.; Ghasemi, S. E. Geotechnical properties of the soils modified with nanomaterials: A comprehensive review. *Arch. Civ. Mech. Eng.* **2017**, *17*, 639−650.
(16) Changizi, F.; Haddad, A. Effect of nano-SiO2 on the geotechnical properties of cohesive soil. *Geotech. Geol. Eng.* **2015**, *34*, 725−733.
(17) Graziani, L.; D'orazio, M. Biofouling prevention of ancient brick surfaces by TiO2-Based nano-coatings. *Coatings* **2015**, *5*, 357−365.
(18) Franzoni, E.; Fregni, A.; Gabrielli, R.; Graziani, G.; Sassoni, E. Compatibility of photocatalytic TiO2-based finishing for renders in architectural restoration: A preliminary study. *Build Environ.* **2014**, *80*, 125−135.
(19) Ouhadi, V. R.; Amiri, M. Geo-environmental behaviour of nanoclays in interaction with heavy metals contaminant, AUT. *J. Civ. Eng.* **2011**, *42*, 29−36.
(20) Melo, J. V. S.; Triches, G. Effects of organophilic nanoclay on the rheological behavior and performance leading to permanent deformation of asphalt mixtures. *J. Mater. Civ. Eng.* **2016**, *28*, No. 04016142.
(21) Taha, M. R.; Taha, O. M. E. Influence of nano-material on the expansive and shrinkage soil behavior. *J. Nanopart. Res.* **2012**, *14*, 1190.
(22) Pham, H.; Nguyen, Q. P. Effects of silica nanoparticles on clay swelling and aqueous stability of nanoparticle dispersion. *J. Nanopart. Res.* **2014**, *16*, 2137.
(23) Iranpour, B.; Haddad, A. The influence of mano-materials on collapsible soil treatment. *Eng. Geol.* **2016**, *205*, 40−53.
(24) Kananizadeh, N.; Ebadi, T.; Rizi, S. E. M.; Khoshniat, S. A. Behavior of nanoclay as an addetive in order to reduce Kahrizak landfill clay permeability. In *2nd International Conference on Environmental Science and Technology*; Singapore, 2011; pp. 55−59.
(25) Taha, O. M. E.; Taha, M. R. Soil-water characteristic curves and hydraulic conductivity of nanomaterial-soil-bentonite-mixtures. *Arab. J. Geosci.* **2016**, *9*, 12.
(26) Baziar, M. H.; Saeidaskari, J.; Alibolandi, M. Effects of nanoclay on the treatment of core material in earth dams. *J. Mater. Civ. Eng.* **2018**, *30*, No. 04018250.
(27) Zahedi, M.; Sharifipour, M.; Jahanbakhshi, F.; Bayat, R. Nanoclay performance on resistance of clay under freezing cycles. *J. Appl. Sci. Environ.* **2014**, *18*, 427−434.
(28) Niroumand, H.; Zain, M. F. M.; Alhosseini, S. N. The Influence of Nano-Clays on Compressive Strength of Earth Bricks as Sustainable Materials. *Procedia-Soc. Behav. Sci.* **2013**, *89*, 862−865.
(29) Mohammadi, M.; Choobbasti, A. J. The effect of self-healing process on the strength increase in clay. *J. Adhes. Sci. Technol.* **2018**, *32*, 1750−1772.
(30) Changizi, F.; Haddad, A. Effect of nanocomposite on the strength parameters of soil. *KSCE J. Civ. Eng.* **2016**, *21*, 676−686.
(31) Govindasamy, P.; Taha, M. R.; Alsharef, J.; Ramalingam, K. Influence of nanolime and curing period on unconfined compressive strength of soil. *Appl. Environ. Soil. Sci.* **2017**, *2017*, No. 8307493.
(32) Niroumand, H., Afsharpour, M., Khaksar, M.. Nano-filler spray strengthing brick monuments, IRPATENT No. 102665, Tehran, Iran, 2020.
(33) Aydin, E. M.; Kara, B.; Bundur, Z. B.; Ozyurt, N.; Bebek, O.; Gulgun, M. A. A comparative evaluation of sepiolite and nano-montmorillonite on the rheology of cementitious materials for 3D printing. *Constr. Build. Mater.* **2022**, *350*, No. 128935.
(34) Qian, Y.; Ma, S.; Kawashima, S.; De Schutter, G. Rheological characterization of the viscoelastic solid-like properties of fresh cement pastes with nanoclay addition. *Theor. Appl. Fract. Mech.* **2019**, *103*, No. 102262.

https://doi.org/10.1021/acsomega.3c00124
ACS Omega 2023, 8, 11373−11380